A sensitivity analysis of the parameters contributing to load development in geogrid pullout testing

David H Marx[1*], and *Jorge G* Zornberg[1]

[1]Masheesh Department of Civil, Architectural and Environmental Engineering, The University of Texas at Austin, Austin, The United States of America

Abstract. A dataset of 334 geogrids pullout tests was analysed to identify the soil and geogrid parameters that have the most significant effect on the rate of load development (K) during pullout. K was calculated for a small displacement of the geogrids and also for a larger displacement. Next a surrogate surface was used to model the relationship between K and parameters representing the geogrid, soil and boundary conditions of the test. Data points sampled from the surrogate surface were used as input to a variance based, global sensitivity analysis. K was found to be the most sensitive to the stiffness of the geogrid, the friction angle of the soil, the spacing of the geogrid ribs, the confining stress and the average particle size. Thus, K is sensitive to the same parameters as the stiffness of the soil-geogrid composite (K_{SGC}). As the K_{SGC} reflects the stiffening function of a geogrid, the load development during pullout is also indicative of the stiffening function of a geogrid.

1 Introduction

Zornberg, Roohi & Gupta introduced an index parameter, the "stiffness of the soil-geosynthetic composite" (K_{SGC}), to quantify the performance of a soil-geogrid composite under serviceability limit state [1]. This index parameter captured both the tensile behaviour of the geogrid and the shear behaviour of the soil while interacting with the geogrid. A strong correlation was found between K_{SGC} and the traffic benefit ratio for model pavements with geogrid-stabilized base layers [2]. Thus, the K_{SGC} was found to be a measure of the stiffening function of geogrids.

The K_{SGC} is derived using a number of simplifying assumptions: 1) the soil-geogrid interaction can be modelled as $dT/dx = -\tau$, where τ is the interface shear stress, 2) J_c is constant for small displacements, and 3) the shear stress along the soil-geosynthetic interface is constant along the active length of the geogrid and zero otherwise. Consequently, the K_{SGC} for a soil-geogrid composite can be defined as: $K_{SGC} = 4 \cdot J_c \cdot \tau_y = T(x)^2/u(x)$, where J_c is the confined stiffness of the geogrid, τ_y is the yield shear stress of the soil, $u(x)$ is the

* Corresponding author: dawie.marx@utexas.edu

displacement of location x along the geogrid during pullout and $T(x)$is the unit tension at that location. Thus, $T(x) = \sqrt{K_{SGC} \cdot u(x)}$.

The K_{SGC} is calculated from the displacement of the internal geogrid nodes during pullout. This study investigated whether the rate of frontal load development (K) in geogrid pullout tests is related to the K_{SGC}. Specifically, the parameters most significant to K were compared to the theoretical definition of the K_{SGC}. If K is related to the K_{SGC} it implies that the rate of frontal load development in a pullout test also reflects the stiffening function of a geogrid.

2 Database

2.1 Rate of load development calculation and distribution

A dataset of 334 pullout load-displacement curves was compiled from literature and prior studies completed by this group [3-19]. All the tests made use of large pullout boxes and were comparable in terms of boundary conditions. For internal clamps, the displacement was reported at the location of the clamp. For external clamps it was reported for geogrid node originally at the mouth of the sleeve. The first quartile (Q_1), median and third quartile (Q_3) ultimate pullout loads (T_{ult}) in the dataset were 21 kN/m, 34 kN/m and 44 kN/m respectively.

The rate of load development (K) during the large pullout tests was defined as $T(x=0)^2/u(x=0)$ to be consistent with the definition of K_{SGC}. $T(x=0)$ and $u(x=0)$ refers to the frontal load and displacement respectively. The K_{SGC} model assumes that $T(x) \propto \sqrt{u(x)}$ over small displacements. However, the typical frontal load-displacement curve of pullout tests has a more complex functional form and $T(x=0)^2/u(x=0)$ is not constant with displacement. Thus, K was calculated for two displacement intervals. The first, $K_{0.25P}$, was calculated as the slope of T^2 versus u, up to the load equal to 25% of T_{ult}. The extension of the geogrid when it was outside of the soil body was found to be insignificant and was thus ignored. The second, $K_{0.5P}$, was calculated up to 50% of T_{ult}.

To smooth the load-displacement curves, a hyperbolic function was fitted up to $0.85 \cdot T_{ult}$ The hyperbolic function was defined as $T = u^a/(b + c \cdot u)$ where a, b and c are fitting coefficients. K was subsequently calculated from the fitted hyperbolic functions. The quality of the fitted curves was evaluated in terms of the $RSME/\sigma$. For hydrological modelling, a ratio of $RSME/\sigma < 0.5$ is considered to be "very good" [20]. For tests where $RSME/\sigma > 0.15$ the hyperbolic model was assumed to be a poor fit to the functional form of the curve. These tests were removed from the dataset. The resulting dataset consisted of 325 tests.

The distributions of $K_{0.25P}$ and $K_{0.5P}$ for the 325 tests are shown in Figure 1. The median displacement increment for $K_{0.25P}$ was 4.8 mm, i.e., a "small" displacement. For $K_{0.5P}$ the median displacement increment was 13.9 mm. The median displacement increments were 7.4% and 21.5% of the median geogrid aperture size in the longitudinal direction (see Section 2.2), respectively.

In Figure 2 the $K_{0.25P}$ is compared with $K_{0.5P}$. There is a strong correlation between the two metrics ($R = 0.87$), indicating that the two variables are internally consistent. However, as the relationship is not perfectly 1:1 it signifies that there is some non-linearity present during load development in pullout tests.

2.2 Geogrids

The dataset comprised of 37 unique geogrids. The most commonly testes geogrids were HDPE, unitized, uniaxial geogrids (36%), followed by PP, extruded, biaxial geogrids (28%) and PET, knitted, uniaxial geogrids (23%). The key geogrid parameters considered for the

analysis were: aperture size in the longitudinal (A_L) and transverse (A_T) directions, the average thickness of the transverse ribs (t_t), and the secant tensile stiffness at 5% axial strain $J_{5\%}$. The ultimate strength of the geogrid (T_{ult}) was not considered for the analysis, as it was strongly correlated to $J_{5\%}$. In addition, $J_{5\%}$ was deemed to be more relevant as K is a measure of load development, rather than strength.

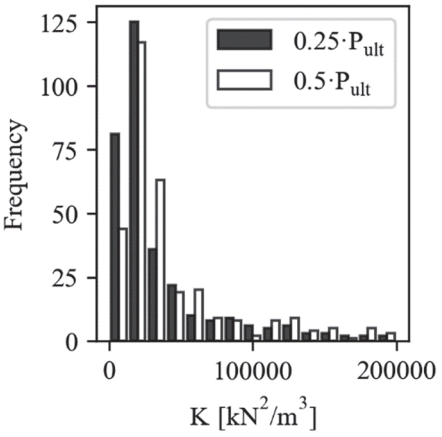

Figure 1. Distribution of K values in the dataset for the two load levels considered.

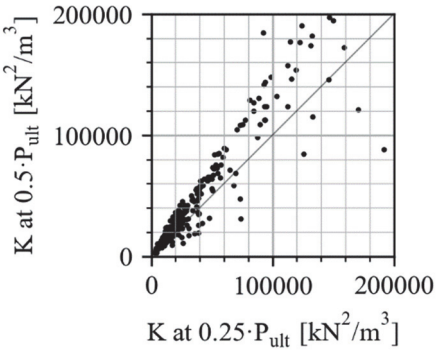

Figure 2. Comparison of the K values calculated for the two load levels

The first quartile, median and third quartile of the geogrid parameters, weighted by the number of tests, is presented in Table 1. In addition, the pairwise correlation of the parameters with $K_{0.25P}$ and $K_{0.5P}$, calculated using Spearman's method, is shown. Spearman's R represents measures a monotonic increase between two variables (not necessarily linear). However, R does not provide any information on the slope of the increase, i.e., the sensitivity, which is the focus of this study.

Table 1. Properties of the geogrids in the dataset

Statistic	**Aperture size [mm]**		t_t **[mm]**	$J_{5\%}$ **[kN/m]**
	A_T	A_L		
Q_1	16.5	36.4	1.4	390
Q_2	27.0	64.6	3.4	618
Q_3	39.3	220	3.9	1034
R with $K_{0.25P}$	-.17	.37	.35	.61
R with $K_{0.5P}$	-.07	.31	.35	.58

2.3 Soils

The database consisted of 30 different soils. The soils ranged from conventional backfill to novel materials such as coal ash, slag and foundry sands. Table 2 presents a summary of the key soil properties considered: D_{50}, the coefficient of uniformity (C_U), the coefficient of curvature (C_Z), the fines content (percentage particles smaller than 0.075 mm, FC) and the Mohr Coulomb parameters for soil strength (ϕ, c). The correlation with $K_{0.25P}$ and $K_{0.5P}$ is also indicated.

The strength parameters are reported for the peak strength where available. For most of the tests, the soil was compacted at the optimum moisture content, i.e., under unsaturated

conditions. Thus, ϕ and c are best regarded as total stress parameters. Only ϕ was considered for the analysis, as it was unclear for several of the tests whether c represented true cohesion or was simply a mathematical construct.

For 78% of the tests the compactive effort was specified in terms of the maximum dry density of the respective soil. For the remaining 22% of tests the compactive effort was specified in terms of the relative density. Nevertheless, for most tests the compactive effort was within 95% of the respective maximum density (whether relative density or MDD).

Table 2. Properties of the soils in the dataset

Statistic	FC [%]	D_{50} [mm]	C_u	C_c	ϕ [°]	c' [kPa]
Q_1	.93	.28	2.42	.88	41.3	0
Q_2	.98	.35	2.85	.97	41.3	1.24
Q_3	6.59	1.54	7.44	1.13	45.3	1.58
R with $K_{0.25P}$	-0.37	.29	.03	.11	.40*	.37
R with $K_{0.5P}$	-0.41	.29	.02	.12	.39*	.31

* Correlation calculated in respect to tan ϕ

3 Methodology

The change in a function y for a local change in input variables x, i.e. dy/dx, is known as the *local sensitivity* of the function. For a non-linear problem, such as pullout resistance, it is often more relevant to evaluate how sensitive y is to the full domain of x, i.e. the *global sensitivity* [19,20]. One type of global sensitivity analyses is variance-based methods. Consider a function y with a distribution of values Y. In a variance-based method the first order effect, S_i, of y to a variable x_i, with distribution X_i is as:

$$S_i = \frac{V_i}{V(Y)} = \frac{Var[E(Y|X_i)]}{Var(Y)} \tag{10}$$

where $Var(\cdot)$ is the variance and $E(\cdot)$ is the expected value. Thus, the first order effect is how much y varies due to X_i when all other variables remain fixed. The concept can be extended to evaluate the sensitivity of y to the interaction to two or more variables, e.g. X_i and X_j. The second order effect can be defined as:

$$S_{ij} = \frac{V_{ij}}{V(Y)} = \frac{Var\left[E\left(y|X_i, X_j\right)\right] - V_i - V_j}{Var(Y)} \tag{11}$$

Finally, the total effect of X_i on y is defined as:

$$S_{Ti} = \frac{V_{Ti}}{V(Y)} = 1 - \frac{Var[E(Y|\boldsymbol{X_{-i}})]}{Var(Y)} \tag{12}$$

where $\boldsymbol{X_{-i}}$ is all variables other than X_i. That is, the sensitivity of y to all possible interactions of X_i, while the other variables remain constant.

To calculate S_{Ti} it is necessary to know the probability distributions of each of the input variables X_i. The 325 datapoints for this study were too few to adequately sample the distributions of twelve variables considered. In addition, the dataset contained some noise that had to be filtered out. Consequently, a surrogate model was fitted to the data to generate synthetic data for the sensitivity analysis.

3.1 Surrogate model

A surrogate model entails reconstructing a non-linear target function, $f(x)$, as the sum of lower order functions centred at known sets of input variables [23], for example:

$$f(x) \approx \sum_{j=1}^{p} w_j \phi_j(x, x_c^j) \tag{13}$$

where ϕ_j is a lower order function centred at the j^{th} set of input variables (x_c^j) and w_j is the weight for ϕ_j. For this study, thin plate splines were used as basis functions: $\phi_j = r^2 \cdot \log r$, with $r = \left\| x - x_c^j \right\|^2$.

Firstly, it was investigated whether the surrogate model can accurately model the relationship between the input parameters ($A_T, A_L, t_T, J_{5\%}, FC, D_{50}, C_U, C_c, \tan\phi, L, \sigma_n$) and K. The surrogate model was fitted to the data using the *SciPy* Python library [24]. Due to the highly non-linear nature of the problem, and the limited size of the dataset, some smoothing was applied when fitting the surface.

The dataset was split into two groups: 87.5% was used for fitting the model and 12.5% for testing the model. To separate the training and testing data, the dataset was stratified into 33 layers ranked on K. Next, one sample was randomly selected out of each layer to create the testing set. Finally, the predictions of the surrogate model for the test dataset were compared with the actual measurements.

The modelled and measured K's for the 31 test points are compared in Figure 3 and Figure 4 for $K_{0.25P}$ and $K_{0.5P}$ respectively. For $K_{0.25P}$ the Root Mean Squared Error ($RSME$) was 7177 kN^2/m^3. For $K_{0.5P}$ it was 8283 kN^2/m^3. For these models the $RSME/\sigma$ were 0.16 and 0.17 for $K_{0.25P}$ and $K_{0.5P}$ respectively. Thus, the surrogate model was deemed to accurately represent the data.

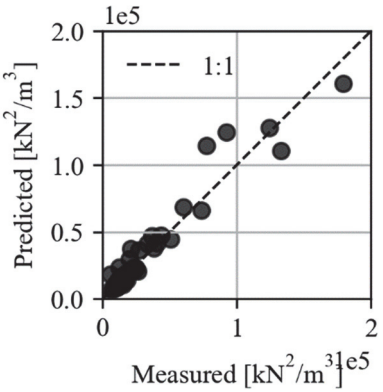

Figure 3. Accuracy of the surrogate model for $K_{0.25P}$.

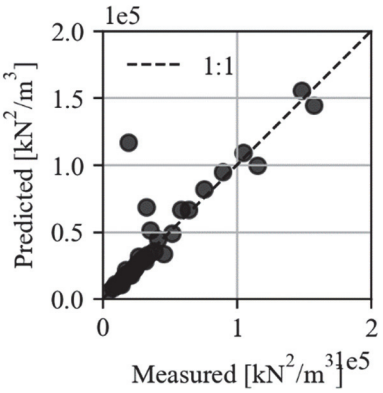

Figure 4. Accuracy of the surrogate model for $K_{0.5P}$.

3.2 Sensitivity analysis

Li et al. proposed a variance based method for global sensitivity analysis in the case of correlated input variables, as is the case for the K [25]. The method entails reconstructing the relationship between Y and X using a random sampling-high dimensional model representation (HDMR). Similar to the surrogate surface in Section 4, the target function is reconstructed as the sum of a series of functions:

$$y \approx f_0 + \sum_{j=1}^{n_p} f_{p_j}\left(\boldsymbol{x}_{p_j}\right) \tag{14}$$

where f_{p_j} are component functions for the contribution of each of the model parameters. Then, the sensitivity of P_R to f_{p_j} can be calculated from the HDMR as:

$$S_{p_j} = \frac{Cov\left(f_{p_j}, P_R\right)}{V(P_R)} = \frac{\sum_{s=1}^{N} f_{p_j}\left(x_{p_j}^{(s)}\right)\left(y^{(s)} - \bar{y}\right)}{\sum_{s=1}^{N}\left(y^{(s)} - \bar{y}\right)^2} \quad (15)$$

Where s refers to the sth sample from the dataset and $\bar{y}$ is the average value of all the $y^{(s)}$'s.

With sufficient data points it would have been possible to apply the HDMR sensitivity analysis directly to the measured data points. However, for this limited dataset it was found best to 1) approximate the dataset with an RBF, albeit with the full dataset, 2) sample random points from the surface following the approach by Saltelli [26] and 3) apply HDMR to the synthetic points. Second order HDMR was applied, that is, the sensitivity of K was calculated with regard to the individual parameters, as well as combinations of parameters.

4 Results

4.1 Sensitivity of pullout stiffness

The sensitivity of $K_{0.25P}$ and $K_{0.5P}$ to the ten most significant parameters is shown in Figure 5 and Figure 6 respectively. Both measures of K were the most sensitive to the friction angle of the soil ($\tan\phi$) (28% and 32% of the total variance, respectively). The second most significant parameter for both measures of K was the stiffness of the geogrid ($J_{5\%}$).

For K calculated over the smaller load range, $K_{0.25P}$, the length of the geogrid tested was significant. When a small displacement is applied to a long geogrid, the active length is considerably shorter than the geogrid. Thus, a substantial section of the geogrid provides anchorage, resulting in lower relative displacement between the geogrid and soil, and a higher K. For $K_{0.5P}$ the larger geogrid displacement results in a relatively insignificant anchorage length. Thus, the lower sensitivity of $K_{0.5P}$ to L.

Both $K_{0.25P}$ and $K_{0.5P}$ were sensitive to σ, as soil stiffness and strength depends on the confining stress. In addition, both $K_{0.25P}$ and $K_{0.5P}$ were sensitive to the aperture size in the longitudinal direction (A_L) and the average particle size (D_{50}). A_L relates to the load transfer between the geogrid and the soil. The closer the transverse ribs are spaced, the more efficient the load transfer. There is, however, a limiting value where the transverse ribs are too close together and interference occurs [27]. The transverse rib spacing, i.e., the load transfer efficiency, affects both the confined stiffness and the interface shear strength.

D_{50} is representative of the shear strength of the soil. In addition, the ratio between D_{50} and A has been found to affect geogrid pullout capacity[28-30]. It is noteworthy that for this dataset, the grading descriptors (C_c and C_z) had a limited effect on the K.

To summarize, the parameters that the K in the dataset was the most sensitive to can be categorized as either 1) relating to the boundary effects of the test: L, 2) relating to the confined stiffness of the geogrid (J_c): $J_{5\%}$, 3) relating to the interface shear strength (τ): $\tan\phi$, D_{50} or 4) relating to both J_c and τ,: σ, D_{50} and A_L. Thus, the load development during a pullout test is sensitive to the same parameters as the K_{SGC}. Consequently, similar to the K_{SGC}, the load development during pullout (K) is representative of the stiffening function of the geogrid. Accordingly, load development during pullout can be used for a first order comparison of the effectiveness of geogrids in stabilizing road base layers.

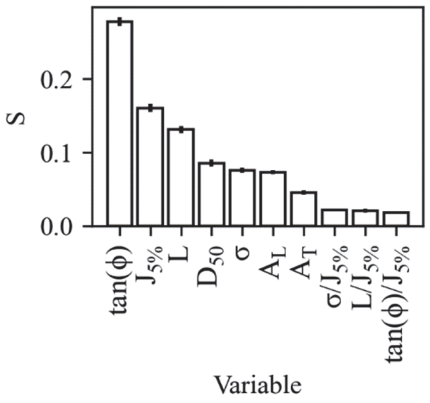

Figure 5. Sensitivity of $K_{0.25P}$ to the ten most significant parameters.

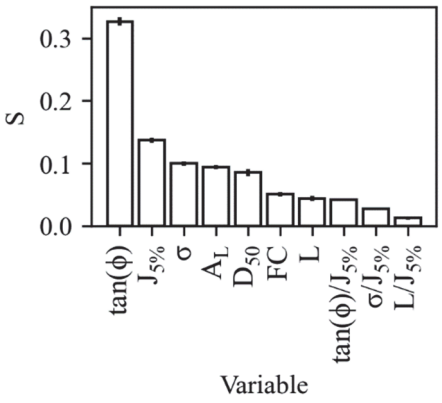

Figure 6. Sensitivity of $K_{0.5P}$ to the ten most significant parameters.

5 Summary

A sensitivity analysis was performed to evaluate the soil and geogrid parameters affecting load development during a pullout test. A dataset of 334 tests was compiled from literature. The load development was quantified as $K = T^2/u$ to be consistent with $K_{SGC} = T(x)^2\ /u(x)$. K was calculated for both a small geogrid displacement and a larger geogrid displacement. Next, a surrogate surface was fitted to this dataset. Randomly sampled points from the surface were used to implement an HDMR sensitivity analysis.

The soil and geogrid parameters that K was sensitive to in the empirical dataset agreed with the theoretical definition of $K_{SGC} = 4 \cdot J_c \cdot \tau$. Firstly, K was the most sensitive to the friction angle of the soil (relating to τ). In addition, K was sensitive to the stiffness of the geogrid (relating to J_c), the confining stress, the average particle size and the spacing of the transverse ribs (relating to both J_c and τ). K was also sensitive to the length of the geogrid, however, that was found to be a boundary effect of the test setup. As K is related to the K_{SGC}, it can be concluded that the load development of a geogrid under pullout is representative of the stiffening function of that geogrid.

The authors thank Tensar International Corporation for the financial assistance provided for the study. Opinions expressed and conclusions presented are solely those of the authors. The first author is grateful for the support provided by a Harrington Dissertation Fellowship. The authors thank Ms Mai-Lyn Zamora for her assistance in digitizing the dataset.

References

[1] J. G. Zornberg, G. H. Roodi, and R. Gupta, J. Geotech. Geoenvironmental Eng. **143**, 10 (2017).
[2] S. Subramanian and J. G. Zornberg, *Predicted performance of geogrid-stabilized unbound aggregate layers using confined soil-geosynthetic composite stiffness*, in Geosynthetics: Leading the Way to a Resilient Planet, Rome, Italy (2023).
[3] M. Alfaro, N. Miura, and D. Bergado, *Geotech. Test. J.* **18**, 2, (1995).
[4] L. S. Calvarano, *Behavior of Different Geogrids under Static and Cyclic Pullout Conditions* (In Italian: Comportamento di Differenti Geogriglie in Condizione di

Sfilamento Statico e Ciclico), PhD Dissertation, Mediterranean University of Reggio Calabria, Italy, (2012).
[5] L. S. Calvarano, G. Cardile, N. Moraci, and P. G. Recalcati, *The influence of reinforcement geometry and soil types on the interface behaviour in pullout conditions*, in Proceedings of the 5th European Conference on Geosynthetics, Spain, (2012)
[6] G. Cardile, N. Moraci, and L. S. Calvarano, Geosynth. Int. **23**, 3 (2016)
[7] M. J. Goodhue, T. B. Edil, and C. H. Benson, *Reuse of foundry sands in reinforced earthen structures,* Environmental Geotechnics Program, University of Wisconsin-Madison, Research Report Report 98-16 (1999)
[8] M. L. Lopes and M. Ladeira, Geotext. Geomembr. **14** 10 (1996).
[9] N. Moraci, D. Gioffre', G. Romano, F. Montanelli, and P. Rimoldi, *Pullout behaviour of geogrid embedded in granular soils* in Proceedings of the 7th International Conference on Geosynthetics, Nice, France, (2002)
[10] N. Moraci and P. Recalcati, Geotext. Geomembr. **24**, 4 (2006)
[11] A. Pant, G. V. Ramana, M. Datta, and S. K. Gupta, J. Clean. Prod. **232** (2019)
[12] A. Pant, M. Datta, G. V. Ramana, and D. Bansal, Measurement, **148** (2019).
[13] P. S. Prasad and G. V. Ramana, Geotext. Geomembr. **44**, 3 (2016)
[14] P. S. Prasad and G. V. Ramana, Geotext. Geomembr. **44**, 4 (2016)
[15] D. M. Raju and R. J. Fannin, Can. Geotech. J., **35** (1998)
[16] G. H. Roodi, *Analytical, Experimental, and Field Evaluations of Soil-Geosynthetic Interaction under Small Displacements*, PhD, The University of Texas at Austin, USA (2016)
[17] A. C. C. F. Sieira, D. M. S. Gerscovich, and A. S. F. J. Sayão, *Geotext. Geomembr.*, **27**, 4 (2009)
[18] S. H. C. Teixeira, *A soil-geogrid interaction study on pullout tests and its application on analysis and designing of reinforced soil structures* (In Portugese: Estudo da interação solo-geogrelha em testes de arrancamento e a sua aplicação na análise e dimensionamento de maciços reforçados) PhD, University of São Paulo, Brazil (2003)
[19] M. R. Abdi and H. Mirzaeifar, Soils Found. **57**, 6 (2017).
[20] D. N. Moriasi, J. G. Arnold, M. W. Van Liew, R. L. Bingner, R. D. Harmel, and T. L. Veith, Trans. ASABE, **50**, 3 (2007).
[21] A. Saltelli *et al.*, Global Sensitivity Analysis. The Primer, 1st ed. Wiley (2007)
[22] T. J. Santner, B. J. Williams, and W. I. Notz, The Design and Analysis of Computer Experiments (2018)
[23] J. A. Snyman and D. N. Wilke, Practical Mathematical Optimization (Springer International Publishing) (2018)
[24] P. Virtanen, R. Gommers, T.E. Oliphant, M. Haberland, T. Reddy, D. Cournapeau, E. Burovski, P. Peterson, W. Weckesser, J. Bright, S.J. Van Der Walt, Nat. Methods **17** (2020)
[25] G. Li., H. Rabitz, P.E. Yelvington, O.O. Oluwole, F. Bacon, C.E. Kolb, J. Schoendorf, J. Phys. Chem. A **114**, 19 (2010)
[26] A. Saltelli, Comput. Phys. Commun., **145**, 2, (2002)
[27] M. R. Dyer, *Observations of the stress distribution in crushed glass with applications to soil reinforcement*, PhD, University of Oxford, Oxford, (1985)
[28] R. W. Sarsby, *The influence of aperture size/particle size on the efficiency of grid reinforcement*, in Proceedings of the second Canadian symposium on geotextiles and geomembranes (1985)
[29] S. F. Brown, J. Kwan, and N. H. Thom, Geotext. Geomembr. **25**, 6 (2007)
[30] B. Han, J. Ling, X. Shu, H. Gong, and B. Huang, *Constr. Build. Mater.* **158** (2018)